JOURNAL OF MATERIALS SCIENCE 33 (1998) 2397–2404

Mechanical properties of calcium- and strontium-substituted lanthanum chromite

S. W. PAULIK, S. BASKARAN, T. R. ARMSTRONG
Pacific Northwest National Laboratory, P.O. Box 999, Battelle Boulevard, Richland, WA 99352, USA
E-mail: T.R. Armstrong@PNL.GOV

Mechanical properties of acceptor (calcium and strontium)-substituted lanthanum chromites are reported as a function of composition, temperature and environment. The strength dependence on temperature for these perovskite conductors was found to depend on the acceptor type, with the calcium-substituted chromites showing a significant reduction in strength with increasing temperature, while the strength of strontium-substituted chromites was essentially invariant with temperature. The decrease in strength observed upon annealing in highly reducing environments was correlated to changes in lattice structure, stoichiometry and fracture morphology. A significant observation was the decrease in the cohesive strength of the grains relative to grain boundaries, beyond a critical oxygen vacancy concentration in the chromites. The structural changes in the chromite lattice upon reduction also resulted in decreased fracture toughness. © *1998 Chapman & Hall*

1. Introduction

Solid oxide fuel cells (SOFCs) with high power density and efficiency are currently being developed for a variety of mobile and stationary power applications. SOFCs are solid-state devices consisting of two porous electrodes (anode and cathode) separated by an ionically conducting electrolyte, typically stabilized zirconia. The electrode materials commonly used are nickel/zirconia cermet for the anode and doped lanthanum manganite for the cathode. The final component is the interconnect which connects the individual cells in series.

The interconnect, which provides the electrical pathway from the anode of one cell to the cathode of the adjacent cell, must be chemically and physically stable in both reducing and oxidizing environments. The interconnect material must be compatible with all other cell components, must be electrically conducting, and have negligible ionic conductivity. In the planar SOFC design, the interconnect is the load-bearing component that supports the other cell components, and must therefore also have adequate strength at high temperature. Only acceptor-substituted lanthanum chromites meet these severe environmental, thermal, and structural requirements.

The fundamental material properties of lanthanum chromite under oxidizing conditions have been measured and reported extensively [1, 2]. However, there has been only limited characterization of the mechanical properties of these materials [3–10]. The flexural strength has been characterized, both at room temperature and high temperature under oxidizing conditions, using three- and four-point sample geometries. In general, room-temperature strength increased with increasing acceptor content; the increase was attributed to an increase in sintered density [3]. The strength of both strontium and calcium-substituted chromites was found to decrease with increasing temperature [4, 5].

Initial investigations into the dependence of the strength on reducing atmospheres have shown mixed results. Milliken *et al.* [6] reported a 50% increase in bend strength of $La_{0.83}Sr_{0.16}CrO_3$ samples after exposure to an oxygen partial pressure ($P(O_2)$) of $\sim 2 \times 10^{-18}$ atm at 1000 °C relative to unexposed samples, whereas Montross *et al.* [7] did not observe any improvement in strength for similar compositions in a reducing (H_2) atmosphere. In addition, Montross *et al.* reported that the bend strength at 1000 °C of $La_{0.85}Sr_{0.15}CrO_3$ and $La_{0.70}Sr_{0.30}CrO_3$ in hydrogen was significantly less than that in air, while $La_{0.80}Sr_{0.20}CrO_3$ was relatively unaffected. Preliminary studies by Paulik and Armstrong [11, 12] have shown significant strength losses after annealing in low-oxygen environments, indicating the need for additional characterization and microstructural control in the lanthanum chromites to ensure adequate long-term performance in fuel-cell environments.

It was the objective of this study to provide an assessment of acceptor (both calcium and strontium)-substituted lanthanum chromite in terms of their mechanical behaviour and performance in application environments. Strength, toughness and elastic properties were characterized as a function of acceptor concentration and temperature, over the range of oxygen partial pressures.

2. Experimental procedure

$La_{1-x}Ca_xCrO_3$ and $La_{1-x}Sr_xCrO_3$ powders (with acceptor concentrations varied from 0.15–0.3) used in this study were synthesized using the glycine-nitrate combustion process (Praxair Specialty Ceramics, Seattle, WA), and then calcined in air at 1000 °C for 1 h. Owing to the high surface area and low packing density of the as-synthesized powder, a processing sequence involving pressing, grinding of the pressed compact, sieving the ground powder through a 150 μm size screen, followed by a final consolidation (isostatic pressing at 276 MPa), was required to obtain high green densities between 65% and 68% theoretical. The green billets, $\approx 34\ mm \times 34\ mm \times 64\ mm$ in size, prepared in this manner were sintered in air between 1600 and 1690 °C for 2–6 h, and then cooled slowly at $2\ ^\circ C\ min^{-1}$ to obtain dense crack-free samples. Selected billets were machined into $3\ mm \times 4\ mm \times 45\ mm$ size bars for flexural tests. Additionally, one billet of each composition was sliced and polished into 10 mm thick square samples, with parallel top and bottom surfaces, for modulus and indentation measurements. Sample densities were measured using the Archimedes' method with ethyl alcohol.

Four-point bend strengths were measured (Instron model 1125) with a crosshead speed of $0.5\ mm\ min^{-1}$ using a fully articulated fixture with a 20 mm inner and a 40 mm outer span. Flexural strengths were measured in air at 25, 600, 800 and 1000 °C. A minimum of ten samples corresponding to each annealing treatment was tested. Samples were heated at approximately 20–25 °C min^{-1} and allowed to equilibrate for 15 min prior to testing.

Selected flexure samples were annealed at 1000 °C in a reducing environment for 2 h, and then tested at room temperature. Samples were first heated to 1000 °C in air in a silica tube furnace and allowed to equilibrate. The gas environment was then controlled with a buffered $CO_2/Ar/H_2$ system metered using mass flow controllers. The use of this system allowed the oxygen partial pressure to be controlled accurately from 10^{-5}–10^{-18} atm. During cooling, constant $P(O_2)$ was maintained to approximately 700 °C.

Fracture toughness was evaluated by the indentation crack-measurement technique [13] for all the $La_{1-x}Ca_xCrO_3$ and $La_{1-x}Sr_xCrO_3$ compositions as a function of the annealing treatment. A 5 kg indentation load (Zwick of America, Inc., E. Windsor, CT) with a 30 s residence time was used. Five indentations and the associated radial cracks, corresponding to each experimental condition were measured and averaged to determine the hardness and fracture toughness. Elastic moduli required for the toughness calculations were obtained on polished samples prior to indentation by the sonic pulse technique [14].

The initial oxygen content of the sintered samples was determined using a potentiometric (oxidation–reduction) titration technique described elsewhere [15]. Samples were then annealed at various oxygen partial pressures for 2 h. After annealing, samples were reoxidized in a thermogravimetric analyser (TGA, Cahn Microbalance). The relative weight changes were measured and corrected for buoyancy effects, and the oxygen content of the annealed samples was determined using the initial oxygen content and the electroneutrality equation.

Scanning electron microscopy (SEM) was used to examine polished sections and fracture surfaces of samples. The grain size was measured using standard stereological techniques described by Underwood [16]. As-sintered and reduced samples were ground to <100 mesh size powder using a mortar and pestle and analysed by X-ray diffraction (Phillips XRG3100). X-ray spectra were collected from 15 °–75 ° 2θ at 0.04 ° increments for 2 s using CuK_α radiation.

3. Results

3.1. Microstructure

For convenience, calcium-substituted lanthanum chromites will be designated by LCC, followed by numerals referring to the amount of dopant added. For example, $(La_{0.8}Ca_{0.2})CrO_3$ is denoted as LCC-20. The average sintered densities of both LSC and LCC samples are listed in Table I. The calcium-doped lanthanum chromite (LCC) samples demonstrated increasing density with increasing acceptor content, similar to previously reported data by Chick *et al.* [17, 18] for strontium additions to lanthanum chromite. The addition of calcium to $LaCrO_3$ allows the formation of a transient liquid phase, $CaCrO_4$ above 1150 °C, which enhances densification [19, 20], resulting in sintered microstructures with grain sizes ranging from 6–9 μm. For the strontium-substituted lanthanum chromite (LSC) samples, densities and average grain sizes were slightly less than similarly doped LCCs, except for the composition with only 16% A-site substitution, which developed a bimodal grain-size distribution.

SEM examination of polished and thermally etched (1200 °C) sections revealed small quantities of a grain-boundary phase in the LSC-20, LSC-24, LCC-20, LCC-25 and LCC-30 samples. It is useful to point out that the thermal etching treatment can cause some exsolution of dopant-rich phases. However, it is likely that even the materials slowly cooled from the sintering temperature are not single phase, because some second phase inclusions are observed in fracture surfaces of samples tested in air at much lower

TABLE I Density, grain size and flexural strength of acceptor-substituted lanthanum chromites

Composition	Theoretical density (%)	Grain size (μm)	Strength (MPa) (25 °C)
LCC-15	87.3 ± 4.5	7.0 ± 1.2	61.0 ± 11.5
LCC-20	94.9 ± 1.6	6.2 ± 1.1	96.0 ± 14.4
LCC-25	96.4 ± 1.9	9.0 ± 1.3	122.7 ± 26.0
LCC-30	97.2 ± 0.5	6.6 ± 0.8	107.4 ± 5.9
LSC-16	93.1 ± 1.5	Bimodal: 2.9 ± 0.4, 46.7 ± 17.2	48.6 ± 10.8
LSC-20	91.6 ± 0.8	3.7 ± 0.8	75.7 ± 8.3
LSC-24	91.2 ± 0.7	4.1 ± 0.7	65.6 ± 9.6

temperatures ($\ll$1000 °C). Energy dispersive X-ray spectroscopy (EDS) revealed calcium-rich phases in fractured surfaces of as-sintered LCC samples, and strontium/lanthanum-rich phases in fractured surfaces of reduced ($P(O_2) = 10^{-16}$ atm, 100 °C) LSC samples. From the polished (thermally etched) cross-sections, it was apparent that LSC samples had more grain-boundary phase than similarly doped LCC samples, especially with the higher acceptor contents. Minor phases, when present in the sintered samples, were below detectable limits by X-ray diffraction. At room temperature, the diffraction patterns revealed only the orthorhombic phase in as-sintered LCCs, and the rhombohedral phase in the LSCs.

3.2. Flexural strength behaviour

3.2.1. Compositional effects on strength

The room-temperature bend strengths of selected LCC and LSC compositions as a function of acceptor content are listed in Table I. The room-temperature strength of the LCC samples increased with increasing calcium content. The density of LCC-15 was only $\approx$ 87% theoretical, so a significant strength improvement was realized by increasing the dopant level to 20% and attaining high sintered density ($\approx$ 95%). Beyond the 25% Ca dopant level, density and strength did not change significantly. The overall observations on density variation with composition shows good agreement with other studies [3]. With the strontium-doped compositions, the strength of the LSC-16 material was limited by the exaggerated grain growth that occurred as a result of a non-uniform distribution of $SrCrO_4$ that forms during sintering. Improved strengths are obtained with higher amounts of dopants (LSC-25 and -30), which promotes liquid-phase sintering and prevents discontinuous grain growth.

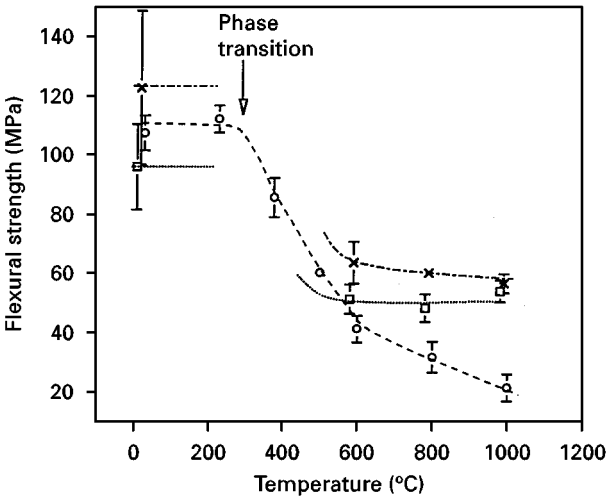

Figure 1 Flexural strength as a function of temperature for calcium-substituted lanthanum chromites: (□) LCC-20, (×) LCC-25, (○) LCC-30.

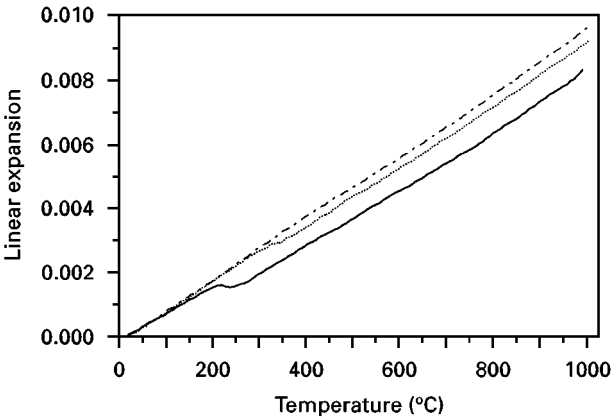

Figure 2 Thermal expansion of acceptor-substituted lanthanum chromites compared to undoped lanthanum chromite: (——) $LaCrO_3$, (·····) LCC-20, (– – –) LSC-20.

3.2.2. Temperature effects on strength

Bend strengths for the LCC (-20, -25 and -30) as a function of temperature are shown in Fig. 1. All LCC compositions showed a decrease in strength at 600 °C relative to room temperature. This is in good agreement with the strength variations recently observed by Montross *et al.* [10] for an LCC-20 material. The strength at low temperatures can be attributed to a progressive decrease in "transformation-toughening" contributions with increasing temperature, since the strength loss with temperature as well as an observed grinding-induced phase transformation phenomenon [10] were similar to the behaviour of transformation-toughened zirconia. This interpretation of the strength behaviour appears to need further investigation. The orthorhombic chromite phase at room temperature is the equilibrium phase, unlike transformation-toughened zirconia where the high-temperature tetragonal phase has to be retained metastably at room temperature for high toughness and strength. In the samples used in this study, no grinding-induced transformation was noted – the phase composition of as-fired, ground and polished surfaces of samples were identical.

A more likely explanation for the strength loss in LCCs with increasing temperature is a decrease in toughness or introduction of strength-controlling flaws due to the phase transition at $\approx$300 °C. Upon heating from room temperature, the LCC compositions undergo a phase transition from orthorhombic to rhombohedral symmetry, similar to undoped $LaCrO_3$ [21, 22]. The phase transformation is detectable by dilatometry, as shown in Fig. 2, where dilatometric traces for 20% acceptor-substituted chromites are compared to undoped $LaCrO_3$. The measured strength at 225 °C is identical to the room-temperature strength, but decreases significantly above 300 °C. The significant decrease across a narrow temperature range at such low temperatures for such an inherently refractory oxide (the lanthanum chromites were considered for high-temperature fibre-reinforcement applications [23]) is most likely due to transformation-weakening, where the phase transition at 250–300 °C results in a high-temperature

rhombohedral phase with lower toughness or defects from the dimensional changes. With further increase in temperature, from 500 °C up to 1000 °C, strength did not change significantly for the LCC-20 and -25 compositions, but the strength of the LCC-30 continued to decrease steadily with temperature. With the highest dopant level (LCC-30), residual calcium-rich second phases can lead to lower strengths with increasing temperature, especially because the test temperatures (800–1000 °C) are a significant fraction ($\geqslant 0.5T_m$) of the melting points of calcium chromate phases [17–19] that form in this system. It is well established that transient low-melting calcium chromate phases form in the calcium-doped chromites [17, 18, 20], and a complex series of reactions control the final phase composition in sintered chromites [19, 20]. A-site dopant levels at 20%–25% are barely adequate for sintering, resulting in almost complete redissolution of the calcium-rich phases into the grains during high-temperature treatment [19], but additional dopant amounts can lead to excess calcium chromate phases. Inspection of the fracture surfaces by SEM confirmed that all the LCC samples tested in air failed by intergranular cracking. But the LCC-30 samples tested at 1000 °C showed significant non-linear deflection behaviour with distinct curvature evident in the broken bars. This is indicative of fracture being preceded by deformation due to low-melting residual second phases at this dopant level.

Bend strengths for the LSCs (-16, -20 and -24) as a function of temperature are shown in Fig. 3. The average four-point bend strengths are in the range 50–80 MPa which are essentially comparable to the 600 °C strengths reported by Sammes and Ratnaraj [8] for LSC-20, after taking into account their use of three-point flexure geometry and a small loading span, which gives higher strengths than the four-point geometry used in this study. The strength of the LSC samples remained unchanged over the entire temperature range from room temperature to 1000 °C. Unlike the LCCs, the rhombohedral phase in the LSCs are stable with increasing temperature, resulting in a constant strength in the low-temperature regime, with no inflection in the thermal expansion (see Fig. 2). At higher temperatures, 600–1000 °C, constant strength is maintained, primarily because of low amounts of residual strontium-rich second phases at the 16%–24% dopant level, and possibly because second phases do not have a significant effect on fracture when the density of the material is only 91%–94% theoretical. This strength retention with temperature for the LSCs is in contrast with the results of Sammes and Ratnaraj [8] who report a decrease in strength by $\approx$ 30%–40% from 600–1000 °C in samples with various compositions (LSC-10, -20 and -30) and densities ($\approx$88%, $\approx$95% and 97% theoretical). Intergranular phases play a major role in controlling strength, and discrepancies in the measured strengths values can arise from the differences in the amounts and composition of these second phases in the test samples at temperature.

3.2.3. Environmental effects on strength

Figs 4 and 5 are plots of the room-temperature strength as a function of $P(O_2)$ for the annealed LCC

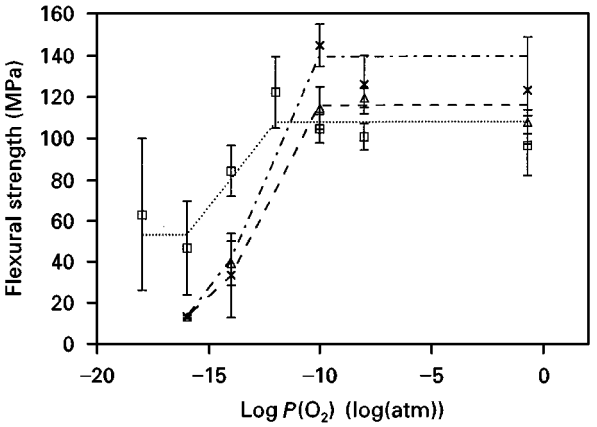

Figure 4 Room-temperature strength of annealed calcium-substituted lanthanum chromites as a function of the oxygen partial pressure used in the 1000 °C heat treatment: (□) LCC-20, (×) LCC-25, (△) LCC-30.

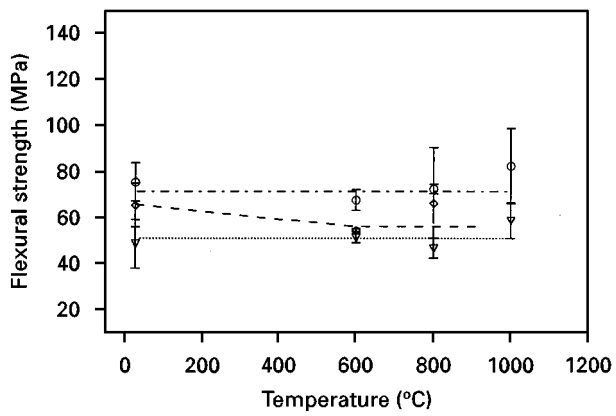

Figure 3 Flexural strength as a function of temperature for strontium-substituted lanthanum chromites: (▽) LSC-16, (○) LSC-20, (◇) LSC-24.

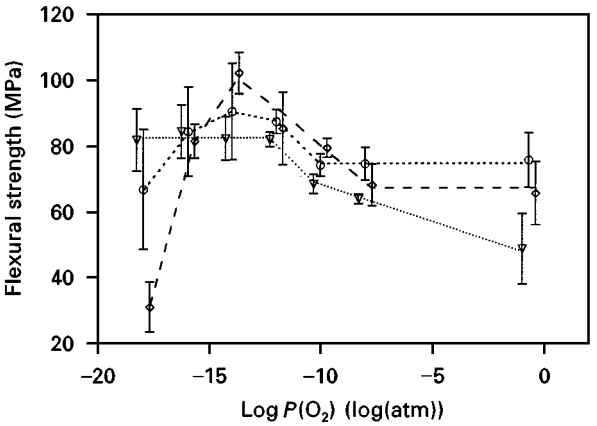

Figure 5 Room-temperature strength of annealed strontium-substituted lanthanum chromites as a function of the oxygen partial pressure used in the 1000 °C heat treatment: (▽) LSC-16, (○) LSC-20, (◇) LSC-24.

and LSC samples, respectively. The results indicate that both acceptor content and type affect the mechanical performance of the material under reducing conditions. With the LCC materials, significant losses in strength were observed after annealing below a critical oxygen partial pressure. The reduction in strength was most significant with the highest dopant level (LCC-30). Furthermore, the loss in strength occurred at higher oxygen pressures with the higher dopant levels. These environmental effects on the strength behaviour are related to structural changes in the chromite lattice (grains), which also results in significant changes in fracture morphology. Scanning electron micrographs in Fig. 6 illustrate a transition in fracture mode, from intergranular to transgranular fracture, that accompanies this decrease in strength observed upon annealing at progressively lower oxygen pressures. It is apparent that the structural changes caused by annealing at very low oxygen partial pressures lowers the cohesive strength of the chromite lattice.

The environmental effects on strength behaviour of LSCs (Fig. 5) are qualitatively similar to that of the LCCs, except much lower oxygen partial pressures are required to affect significantly the retained strength. A slight increase in strength is observed with decreasing oxygen pressure in the annealing treatment, before strengths begin to decrease after very low oxygen heat-treatments. Again, the materials with higher dopant levels begin to show strength losses after annealing at higher oxygen pressures. The fracture surfaces illustrated in Fig. 7 also indicate that structural changes in the lattice upon annealing at low oxygen environments results in lower grain strengths, i.e. cohesive strength in the chromite lattice is reduced, leading to transgranular fracture. The theoretical cohesive strength of the lattice is controlled by the fracture energy and the elastic modulus of the material [24], both of which can also undergo changes with annealing at low oxygen pressures.

3.3. Fracture toughness and elastic modulus

The variation in indentation fracture toughness with annealing treatment for LSC (LSC-24) and an LCC (LCC-25) samples are shown in Fig. 8. Prior to heat treatment, the fracture toughness of the as-sintered LSC sample was $\approx 1.1\,\mathrm{MPa\,m^{1/2}}$, and the LCC material $\approx 2.1\,\mathrm{MPa\,m^{1/2}}$. Similar to the flexural strength, the average toughness decreased significantly below a critical oxygen pressure. The indentation cracks also showed, in general, more intergranular fracture after high oxygen pressure treatments, and evidence of transgranular fracture after heat treatments at very low oxygen pressures, indicating that structural changes in the lattice also lowers the fracture surface energy of the perovskite

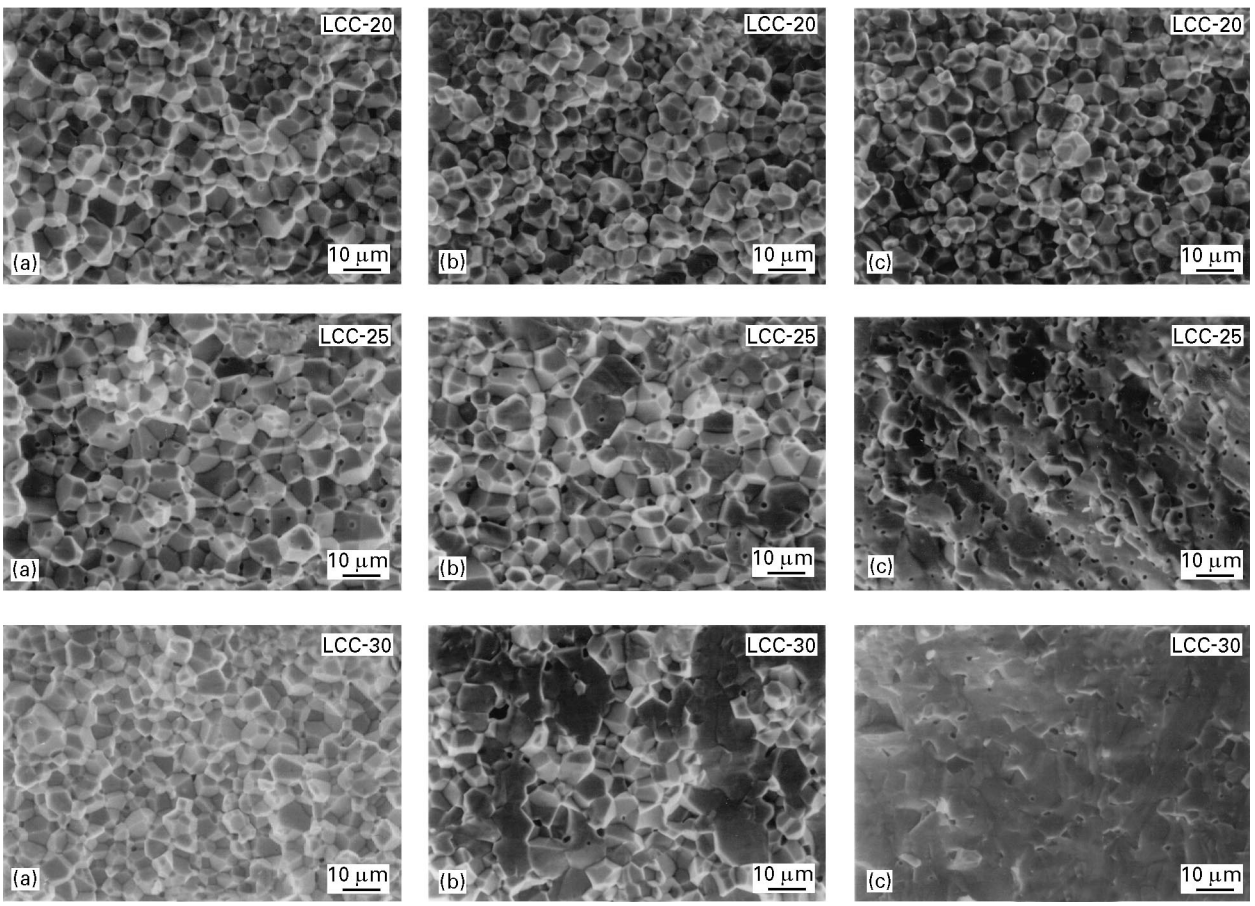

Figure 6 Scanning electron micrographs of fracture surfaces of annealed calcium-substituted lanthanum chromite bar specimens. Samples annealed in (a) air, (b) 10^{-10} atm $P(O_2)$ and (c) 10^{-16} atm $P(O_2)$. Note the transition from intergranular to transgranular fracture with decreasing oxygen partial pressures in the annealing treatment.

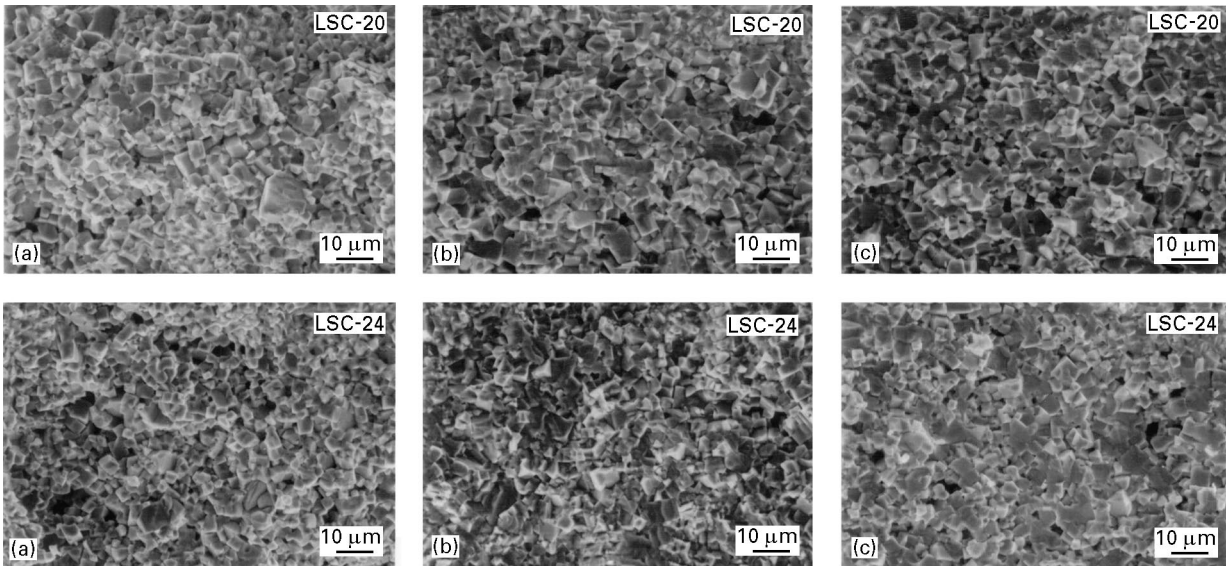

Figure 7 Scanning electron micrographs of fracture surfaces of annealed strontium-substituted lanthanum chromite bar specimens. Samples annealed in (a) air, (b) 10^{-14} atm $P(O_2)$ and (c) 10^{-18} atm $P(O_2)$. Note the transition from intergranular to transgranular fracture with decreasing oxygen partial pressures in the annealing treatment.

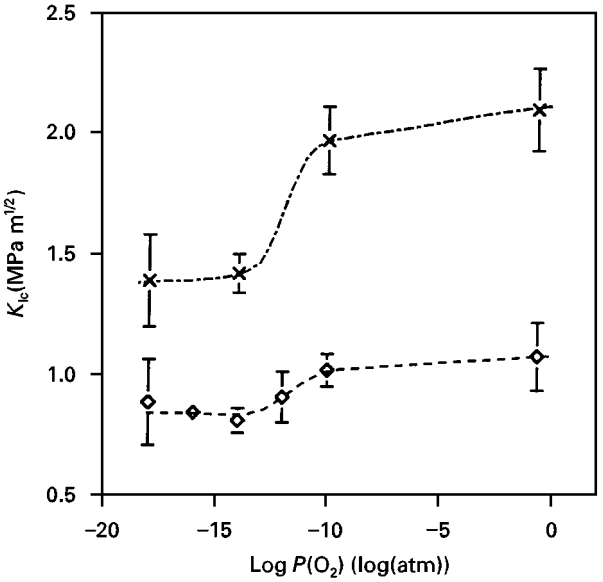

Figure 8 Indentation fracture toughness of annealed (◇) LSC-24 and (×) LCC-25 samples as a function of oxygen partial pressures used in the annealing treatment.

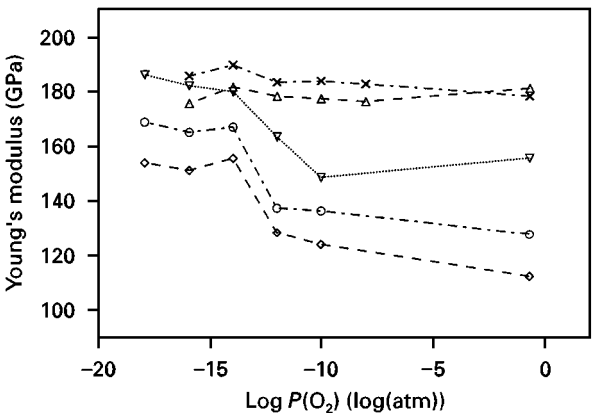

Figure 9 Elastic modulus of annealed calcium and strontium-substituted lanthanum chromites as a function of oxygen partial pressures used in the annealing treatment: (▽) LSC-16, (○) LSC-20, (◇) LSC-24, (×) LCC-25, (△) LCC-30.

grains. This behaviour showing decreased fracture toughness after heat treatments at low oxygen pressures, is similar to the fracture behaviour observed in Y_2O_3 [25] where K_{Ic} was found to decrease by $\approx 30\%$ after annealing at 1700 °C for 2 h in a vacuum of ≈ 13.3 kPa. For the reduced yttria material, the lower toughness was correlated to a high concentration of oxygen vacancies, and reduced ionic character of the Y–O bond which lowers the bond strength.

The elastic modulus for both LCC and LSC materials is shown in Fig. 9 as a function of oxygen partial pressures in the annealing treatment. Slight increases in modulus for the LSCs were observed upon annealing at low oxygen pressures, while the elastic moduli of the LCC materials were essentially invariant with annealing treatment, indicating that structural changes to the lattice predominantly affect only the fracture surface energy and the mechanical strength.

4. Discussion

The variations in strength, toughness and fracture morphology with these annealing treatments arise from structural changes in the chromite lattice, which also affect the thermal expansion behaviour and dimensional stability of these materials [15, 26]. It has been noted that doped lanthanum chromite samples exhibited increasing expansion below a critical oxygen pressure, with the onset of expansion occurring at a higher $P(O_2)$ for compositions with higher acceptor content [26]. Similarly, the magnitude of the expansion after a specific annealing treatment was greater in samples with higher acceptor contents.

In reducing environments at high temperatures, oxygen is lost from the chromite lattice, resulting in the formation of oxygen vacancies, and reduction of Cr^{4+} to Cr^{3+} to provide charge compensation. For

LCC-30, the mole fraction of Cr^{4+} is reduced from 0.26 to 0.06 [26]. Armstrong *et al.* [26] have argued that the lattice expansion ($\approx 1.3\%$) upon reduction is primarily because of the change in ionic radius of chromium (0.055 nm to 0.062 nm) associated with the change in the chromium oxidation state ($4+$ to $3+$). The increased ionic size from the annealing treatment can also potentially decrease the strength of the chemical binding, or the cohesive strength of the lattice. Accurate prediction of fundamental strengths of these oxides awaits rigorous molecular dynamics calculations, but to a rough approximation, the strength of chemical binding in simple oxide structures can be assessed from the cationic field strengths computed at the oxygen sites of the lattice [27]. A simple calculation of the coulombic force can be performed for the Cr–O bond. The field strength is proportional to Z/R^2 where Z is the cationic charge, and R is the interatomic distance, $r_{Cr} + r_O$. The field strength (2.10×10^2 e nm^{-2} with chromium in the $4+$ state, and 1.47×10^2 e nm^{-2} with chromium in the reduced $3+$ state, using ionic radii values for a coordination number of 6 [28]. The significant difference in the estimated field strength between the different chromium oxidation states for this simple case suggests that the cohesive strength of the more complex chromite lattice could also change significantly when Cr^{4+} is reduced to Cr^{3+} during annealing. While this calculation of field strengths provides some insight on why cohesive strength of chromites can decrease with reduction, it fails to explain the small increase in strength observed in LSCs on reduction. The observed increase in strength in LSCs may arise from changes in the grain-boundary structure, and needs further investigation by transmission electron microscopy.

The decrease in strength and fracture toughness upon annealing in reducing atmospheres could also depend on the distribution of oxygen vacancies in the lattice. Strength and fracture toughness as a function of the oxygen stoichiometry (number of oxygen ions per formula unit) are plotted in Figs 10 and 11. The data for both unannealed and annealed samples are included in the plots. For clarity, the strength data for only two compositions are shown. The toughness data fall into two groups, with the lower values corresponding to the highly reduced samples, while the strength decreases with increasing oxygen vacancy concentration. Because the reduced samples show predominantly transgranular fracture, it appears that oxygen vacancies in small (overall) concentrations can affect the crack propagation characteristics through the lattice. The modulus is not changed significantly by the annealing treatment, thus the ratio of fracture toughness to modulus is lowered by the formation of oxygen vacancies. For other materials where this ratio is low, the fracture behaviour is believed to be controlled by the easy cleavage fracture along specific crystallographic planes of the lattice [29]. Further characterization by electron microscopy and scattering techniques is required to determine whether preferred fracture paths through the grains could result from ordering of oxygen vacancies in these chromites.

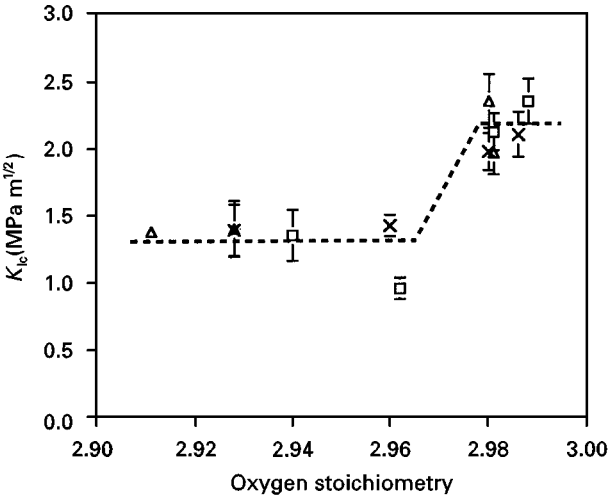

Figure 10 Indentation fracture toughness of calcium-substituted lanthanum chromites as a function of oxygen stoichiometry (y in $La_{1-x}Ca_xCrO_y$): (□) LCC-20, (×) LCC-25, (△) LCC-30.

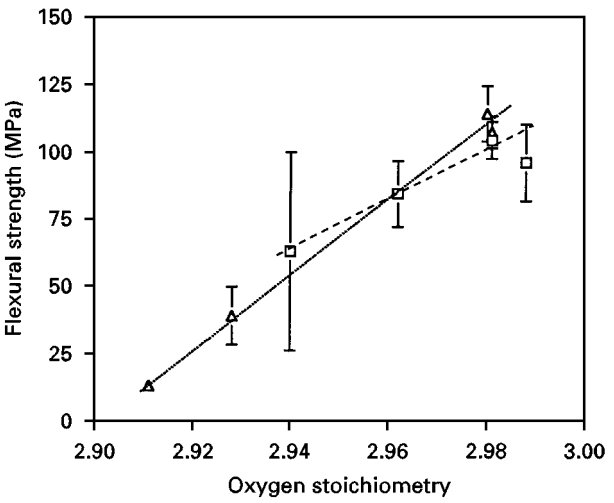

Figure 11 Room-temperature strength of calcium-substituted lanthanum chromite ((□) LCC-20 and (△) LCC-30) as a function of oxygen stoichiometry (y in $La_{1-x}Ca_xCrO_y$).

5. Conclusion

Strength behaviour of acceptor-substituted lanthanum chromites depends on acceptor type and amount. The flexural strength of calcium-substituted chromites decreases with temperature, even at low temperatures, while strontium-doped chromites show no change in strength over a wide temperature range. Annealing acceptor-substituted chromites at low oxygen partial pressures results in significant decreases in strength, as a result of structural changes to the lattice that accompany the reduction of Cr^{4+} to Cr^{3+} and formation of oxygen vacancies. In reduced chromites, cracks preferentially propagate through grains. A lower fracture surface energy is inferred from the decreased fracture toughness measured after the annealing treatment at low oxygen partial pressures.

Acknowledgements

The authors thank R. Kurosky, D. McCready and J. Young for their experimental assistance. This work

was sponsored by the US Department of Energy's Morgantown Energy Technology Center under Contract 22407. Pacific Northwest National Laboratory is operated for the US Department of Energy by Battelle Memorial Institute under contract DE-AC06-76RLO 1830.

References

1. N. Q. MINH and T. TAKAHASHI, in "Science and Technology of Ceramic Fuel Cells" (Elsevier, Amsterdam, 1995).
2. N. Q. MINH, *J. Amer. Ceram. Soc.* **76** (1993) 563.
3. N. M. SAMMES, R. RATNARAJ, and M. G. FEE, *J. Mater. Sci.* **29** (1994) 4319.
4. M. MORI, H. ITOH, N. MORI and T. ABE, in "Proceedings of the 3rd International Symposium on Solid Oxide Fuel Cells", edited by S. C. Singhal and H. Iwahara (The Electrochemical Society, Pennington, NJ, 1993) p. 325.
5. N. M. SAMMES, R. RATNARAJ and C. E. HATCHWELL, in "Proceedings of the 4th International Symposium on Solid Oxide Fuel Cells (SOFC-IV)", edited by M. Dokiya, O. Yamamoto, H. Tagawa and S. C. Singhal (The Electrochemical Society, Pennington, NJ, 1995) p. 952.
6. C. MILLIKEN, S. ELANGOVAN and A. KHANDKAR, in "Proceedings of the 3rd International Symposium on Solid Oxide Fuel Cells", edited by S. C. Singhal and H. Iwahara (The Electrochemical Society, Pennington, NJ, 1993) p. 335.
7. C. S. MONTROSS, H. YOKOKAWA, M. DOKIYA and M. ANZAI, in "Extended Abstracts of the 60th Meeting of the Electrochemical Society of Japan", (1993) p. 263.
8. N. M. SAMMES and R. RATNARAJ, *J. Mater. Sci.* **30** (1995) 4523.
9. C. S. MONTROSS, H. YOKOKAWA, M. DOKIYA and L. BEKESSY, *J. Amer. Ceram. Soc.* **78** (1995) 1869.
10. C. S. MONTROSS, H. YOKOKAWA and M. DOKIYA, *Scripta Mater.* **34** (1996) 913.
11. S. W. PAULIK and T. R. ARMSTRONG, in "Program and Abstracts of the 1996 Fuel Cell Seminar", Orlando, FL, November 1996, p. 131.
12. S. W. PAULIK and T. R. ARMSTRONG, in "Proceedings of the 2nd European Symposium on Solid Oxide Fuel Cells", edited by B. Thorstensen (European Solid Oxide Fuel Cell Forum, Oberrohrdorf, Switzerland, 1996) p. 547.
13. G. R. ANSTIS, P. CHANTIKUL, B. R. LAWN and D. B. MARSHALL, *J. Amer. Ceram. Soc.* **64** (1981) 533.
14. E. SCHREIBER, O. L. ANDERSON and N. SOGA, in "Elastic Constants and Their Measurement" (McGraw-Hill, New York, 1973).
15. T. R. ARMSTRONG, J. W. STEVENSON, D. E. MCCREADY, S. W. PAULIK and P. E. RANEY, *Solid State Ionics* **92** (1996) 213.
16. E. R. UNDERWOOD, in "Quantitative Stereology" (Addison-Wesley, Reading, MA, 1970).
17. L. A. CHICK, J. L. BATES and G. D. MAUPIN, in "Proceedings of the 2nd International Symposium on Solid Oxide Fuel Cells", edited by F. Grosz, P. Zegers, S. C. Singhal and O. Yamamoto (Commission of the European Communities, Luxembourg, 1991) p. 621.
18. J. L. BATES, L. A. CHICK and W. J. WEBER, *Solid State Ionics* **52** (1992) 235.
19. L. A. CHICK, J. LIU, J. W. STEVENSON, T. R. ARMSTRONG, D. E. MCCREADY, G. D. MAUPIN, G. W. COFFEY, and C. A. COYLE, *J. Amer. Ceram. Soc.* (1996).
20. N. SAKAI, T. KAWADA, H. YOKOKAWA, M. DOKIYA and I. KOJIMA, *ibid.* **76** (1993) 609.
21. C. P. KHATTAK and D. E. COX, *Mater. Res. Bull.* **12** (1977) 463.
22. M. MORI, T. YAMAMOTO, H. ITOH and T. ABE, in "Proceedings of the 4th International Symposium on Solid Oxide Fuel Cells (SOFC-IV)", edited by M. Dokiya, O. Yamamoto, H. Tagawa and S. C. Singhal (The Electrochemical Society, Pennington, NJ, 1995) p. 905.
23. E. L. COURTRIGHT, H. C. GRAHAM, A. P. KATZ and R. J. KERANS, WL-TR-91-4061, Wright Patterson Air Force Base, OH (1992).
24. S. M. WIEDERHORN, in "Mechanical and Thermal Properties of Ceramics", edited by J. B. Wachtman, Jr., National Bureau of Standards (US) Special Publication **303** (National Bureau of Standards, Washington, DC, 1969) p. 217.
25. G. FANTOZZI, G. ORANGE, M. GAUTIER, J. P. DURAUD, P. MAIRE, C. LEGRAUSS and E. GILLET, *J. Amer. Ceram. Soc.* **72** (1989) 1562.
26. T. R. ARMSTRONG, J. W. STEVENSON, L. R. PEDERSON, and P. E. RANEY, *J. Electrochem. Soc.* **143** (1996) 2919.
27. W. B. HILLIG, *J. Amer. Ceram. Soc.* **76** (1993) 129.
28. R. D. SHANNON, *Acta Crystallogr.* **A32** (1976) 751.
29. R. RICE, *J. Mater. Sci.* **31** (1996) 4503.

Received 31 January 1997
and accepted 27 January 1998